7th International Conference & Exposition on Petroleum Geophysics

"HYDERABAD 2008"

P - 293

Time-lapse Inversion for Monitoring In-situ Combustion Process in Balol Field, India

Asit Kumar*, N Bhattacharyya & H.L. Kharoo

Institute of Reservoir Studies, ONGC, Ahmedabad, India, Email: kumar_asit@hotmail.com

Summary

The present study deals with post-stack inversion of time-lapse 3D data for monitoring in-situ combustion process in a pilot area of Balol Field of Cambay basin, India. The base 3D dataset pertains to survey conducted prior to the commencement of in-situ combustion process in the already identified set of injector wells. The monitor 3D survey was carried out 12 months thereafter for studying the changes in the reservoir due to this thermal process. The two data sets were acquired with the same acquisition parameters and processed identically. We performed post-stack inversion of these 3D datasets to arrive at clear 4D anomalies in terms of impedance that could be meaningfully interpreted and validated with reservoir engineering and production data. Although various inversion workflows were applied, 4D impedance anomalies are best seen in case of inversion of cross-equalized datasets through a matching procedure using identically processed PSTM gathers. The possible fairways of flue gases and/or propagation of combustion have also been brought out through attribute studies. The study indicates the preferential movement of flue gases towards north through the finer N-S discontinuities. This observation is supported by production behavior of wells in the area.

Introduction

Time-lapse seismic relies on careful matching of multiple 3D seismic surveys that image the reservoir at different calendar times to monitor the changes due to production/injection in the reservoir. It is now well established as a reliable reservoir monitoring technique that certainly adds value to the reservoir management (Landro, 2006).

Time-lapse analyses are essentially qualitative as long as seismic vintage comparison is restricted to seismic amplitude changes. There is however a strong need to transform these seismic variations into quantitative production-related changes (Gluck, 2000). Inversion of time-lapse data provides a quantitative link between amplitude change and the physical changes that have occurred in the reservoir due to production. Acoustic impedance inversion converts post-stack seismic data from amplitudes to acoustic impedance. In order to estimate changes in reservoir properties, it is important to obtain reliable impedance models through 4D data inversion (Sarkar, 2003). This paper describes the results from post-stack inversion of time-lapse data.

There are a number of approaches to time-lapse inversion. Most commonly, it can be formulated as a natural extension of 3D inversion, where different vintages are inverted separately and the results are subtracted to obtain changes in elastic parameters (Buland et al, 2006). There can be several workflows depending on the data and methods used to perform the inversion. In this study, we carried out post-stack inversion using different methods on matched as well as unmatched but identically processed datasets followed by differencing to extract time-lapse acoustic impedance anomalies for comparison and analysis. The objective has been to bring out clear time-lapse impedance anomalies for reliable interpretation and integration with reservoir/production data.

The time-lapse data for this study pertains to northern part of Balol Field, situated in the heavy oil belt of Mehasana block, Cambay basin, India (Fig.-1). The major hydrocarbon–bearing sand in the area is KS-1 sand of Middle Eocene age at a depth of about 1000m, mostly unconsolidated with porosity in the range of 25-30 % and permeability varying between 1-5 darcies. The primary recovery of viscous oil from Balol Field is about 13%. In-situ combustion process is being carried out in parts of the field on commercial scale for improving the recovery of oil from the reservoir. a time-lapse study was planned in a small pilot area of 0.96x1.36 sq. km. in the northern part of Balol Field to track the movement of thermal front and estimation of areal sweep for the placement of future injector and producer wells. A feasibility study based on Gassmann fluid substitution and seismic forward modeling was carried out to estimate the change in seismic properties and assess the detectability of time-lapse signal. The study indicated that in-situ combustion process can give rise to an observable change in seismic response due to substantial decrease in impedance in the combustion zone/gas zone and thus it would be possible to monitor the thermal EOR in successive repeat surveys (Asit Kumar & Shyam Mohan, 2004). Following this, baseline and monitor 3D surveys were designed, acquired, processed and finally cross-equalized with the above mentioned objective for 4D study (Asit Kumar, N. Bhattacharyya and Shyam Mohan, 2006).

Base 3D data, representing pre-combustion stage, was acquired during Oct-Nov, 2003 with a bin size of 10mx10m and nominal fold of 36. After the acquisition of base 3D data was over, four wells in the area (Fig.-2) were put on in-situ combustion successively from north to south. A repeat (monitor) 3D survey was carried out 12 months later under similar climatic conditions with same survey parameters. The basic processing of base and monitor datasets was carried out in the identical manner. Finally, both the datasets were subjected to pre-stack time migration and the resulting PSTM gathers cross-equalized to derive meaningful 4D amplitude anomalies around injector wells (Asit Kumar et al, 2006).

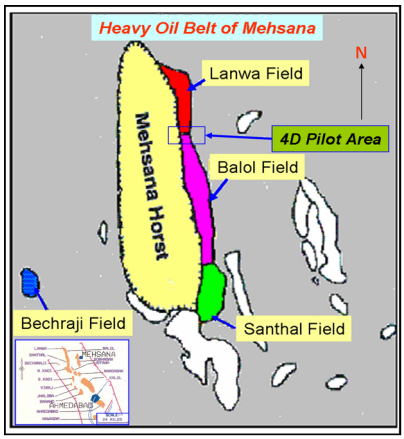

Figure 1: Location map of Balol Field, Cambay Basin, India. The area of time-lapse study is marked by the blue rectangle in the northern part of the field.

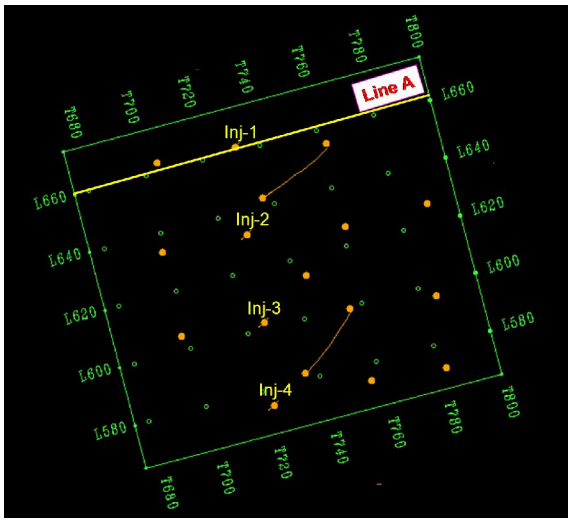

Figure 2: Area of study with injector wells.

Method

Time-Lapse Inversion

As mentioned earlier, time-lapse inversion can be performed in several ways. We followed two workflows of time-lapse inversion. In the first workflow, the original identically processed data sets are inverted with a common wavelet separately and then differenced. In the second, time-lapse seismic processing is followed by inversion of cross-equalized base and monitor datasets with a common wavelet. The wavelet and initial guess model for inversion were derived using available well-log information in addition to seismic data. In each of the workflows the inversion was carried using model-based as well as sparse-spike methods. The resulting impedance data after all these

inversions were compared and analyzed to assess the efficacy of different inversion procedure in producing the desired 4D impedance signal. Although the inversion was run on the entire 3D volume, we present the results, without loss of generality, along a cross-section only (Line A) passing through one of the injectors (Inj-1) in the area.

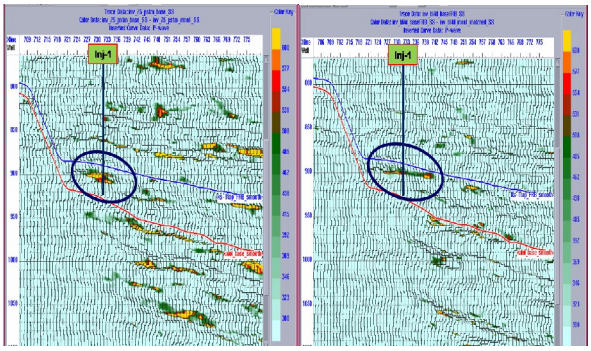

Figure 3: Impedance difference section along Line A obtained from post-stack sparse-spike inversion of PSTM base and monitor data (left) and matched base and monitor data (right).

Fig.-3 shows 4D impedance difference sections passing through injector well Inj-1after post-stack sparse-spike inversion on initial identically processed base and monitor PSTM datasets and on matched monitor and base datasets. The panel on the left pertains to acoustic impedance difference obtained after differencing the output of inversion from PSTM volumes while the panel on the right refers to the impedance difference of that of matched volumes. The impedance difference on the right in Fig.-3 reveals a 4D response at the location of injector well. Moreover, the undesirable differences due acquisition/processing present in the panel on the left have also been considerably reduced making the section less noisy.

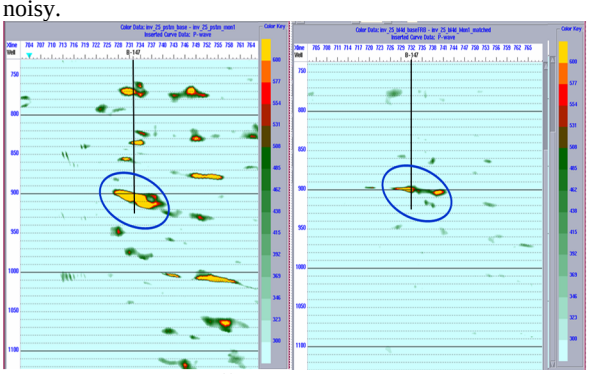

Figure 4: Impedance difference section along Line A obtained from model-based inversion of PSTM base and monitor data (left) and matched base and monitor data (right).

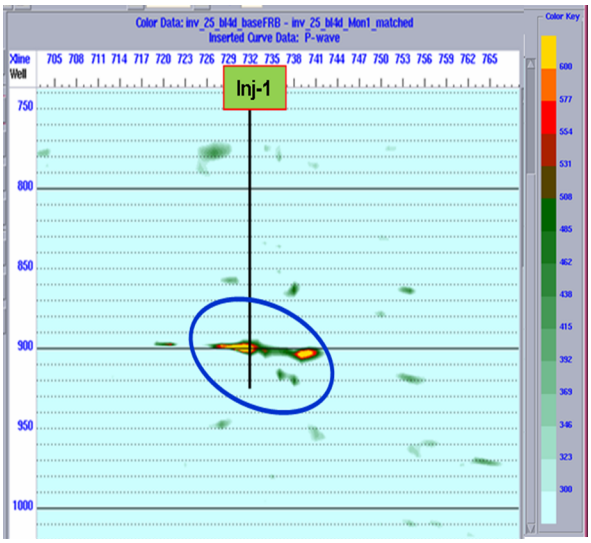

Figure 5: 4D impedance difference section passing through well Inj-1.

The results of model-based inversion on PSTM datasets and 4D-processed matched datasets are depicted after differencing the inversion outputs in Fig.-4. Here, again the acquisition/processing-related residual differences have overwhelmed the background on the left panel making it difficult to identify the 4D signal unambiguously. However, the panel on the right pertaining to differenced output of matched datasets has distinctly and unambiguously brought out the lowering of impedance at the injector well. The noises have been minimized too in this inversion.

Fig.-5 is a zoomed map of the panel shown on the right of Fig.-3. The color scales in these maps are identical for maintaining consistency in comparison.

Interpretation and Analysis

A comparison of Figs.-3 and 4 shows that model-based inversion has proved more effective than sparse-spike method in isolating the 4D effect due to combustion inside the reservoir. It is also evident that the ambiguity in deciphering 4D signal can appreciably be reduced when different vintage datasets are processed in 4D sense prior to carrying out the inversion. However, inversion itself and consequently the 4D difference signal is also sensitive to wavelet, initial guess model and the inversion algorithm followed in a particular workflow. Therefore, some uncertainty in estimation and quantification of 4D signal may be attributed to the inherent non-uniqueness of inversion itself.

Similar 4D anomalies were also observed at other locations of injectors (Inj-2, 3 and 4) although with varying degree and extent. To see the effect of gas/air injection and their

possible fairways in terms of decrease in impedance, RMS envelope attribute was extracted from impedance difference volume in a window along and inclusive of KS-1 sand top. Fig.-6 depicts this attribute where higher values of impedance difference meaning larger decrease in impedance with respect to base survey is clearly visible in the vicinity of injectors. This 4D difference anomaly may be compared with somewhat noisier but similar pattern indicated by average absolute amplitude attribute derived from amplitude difference volume in Fig.-7.

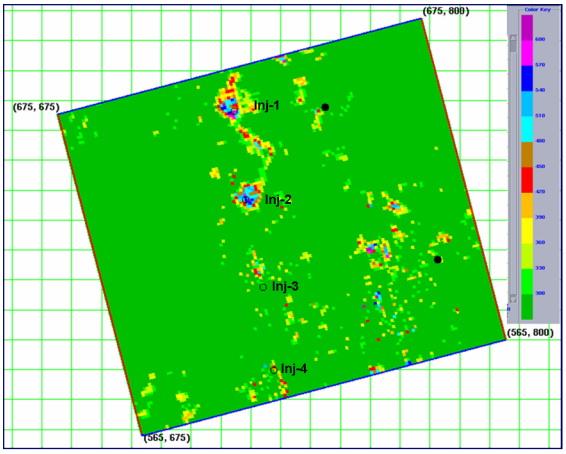

Figure 6: RMS envelope attribute in a window of 24 ms below KS-1 Top time horizon derived from impedance difference cube.

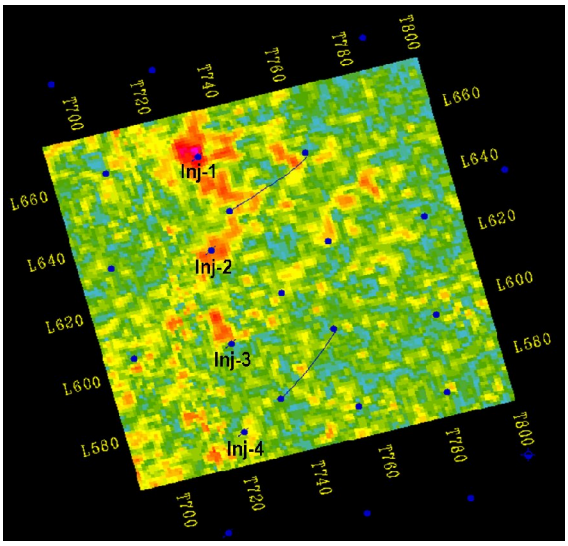

Figure 7: Average absolute amplitude in a window of 24 ms below KS-1 Top time horizon derived from amplitude difference cube.

The impedance anomalies seen around injector wells is a collective response of burnt zones of different sizes/extent having gases trapped inside the reservoir at these well locations and varying flue gas saturations along the gas migration path. It is readily seen that the combustion in these wells are not uniform. The shape and orientation of these anomalies point to preferred path of gas/front movement. Moreover, 4D anomalies are most conspicuously visible in Inj-1 and Inj-2 wells only. In Inj-3 and Inj-4, the 4D anomalies have weakened considerably and are only marginally above the background indicating that combustion was not effective enough to produce a significant response. The maximum combustion appears to have taken place around Inj-1 well, resulting in the most pronounced response at this well. This observation is also supported by a plot of air injection rate of the injection wells given in Fig.-8. Evidently, Inj-1 received the highest air injection (shown in magenta color) thereby sustained a much better and higher level of combustion than in other wells.

Fluid substitution 1D modeling using Gassmann equation to logs of a well nearby Inj-1 indicates an impedance drop of about 14-15% for a change from initial (in-situ) saturation condition to fully saturated (100%) gas over the complete interval of reservoir (KS-1 sand) in the injector well which can be expected in the case of completely burnt zone devoid of any oil or water. However, the decrease in impedance as observed around injector wells Inj-1 & 2 in Fig.-6 is generally in the range of 7-10% implying somewhat lesser reduction than the modeled value but still giving rise to a good impedance contrast.

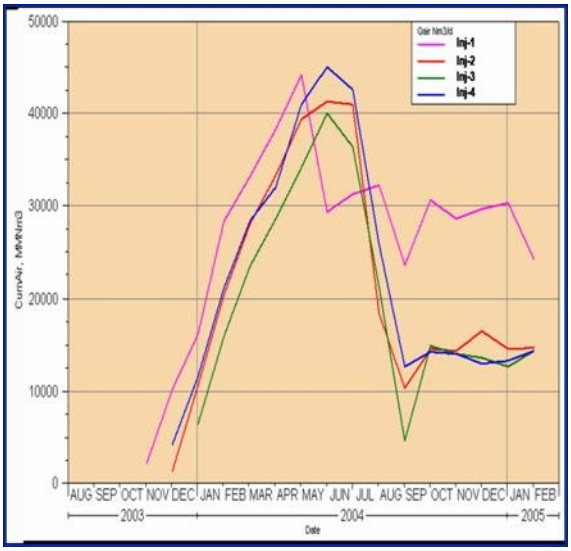

Figure 8: Month wise rate of air injection in the injector wells.

It can clearly be seen from attribute maps (Figs 6-7) that the flue gases have tended to move preferentially in the N-S and NE-SW direction. Both these attributes suggest a possible migration of gas and therefore, injection effect northwards to the adjoining Lanwa Field. Spectral decomposition was also carried out using KS-1 top time horizon. Fig.-9 is one such spectral slice at 22Hz frequency exhibiting a prominent N-S running major fault in the area marked '**F1**' and other finer smaller faults/discontinuities seen as various lineaments in white streaks in the map. Envelope of RMS impedance attribute from impedance difference volume is superimposed on this spectral slice in Fig.-10. Note that the 4D anomalies are found to almost align over spectral lineaments (Fig.-10) indicating the movement of thermal front/combustion gases along the fault zone/discontinuities towards north. This preferential transmission of thermal energy seems to have given rise to increase in oil production and decrease in water cut in some well lying close to the fairway shown in spectral slice (Figs. 9-10). The production behavior of two such wells L-A and L-B corroborates this observation where oil rates have gone appreciably up after start of ignition and during the continuance of air injection in the injectors lying south of these production wells. In fact, the water cut map prepared on the basis of reservoir engineering data for pre- and post-combustion scenario (Fig.-13) further validates the observations from 4D analysis.

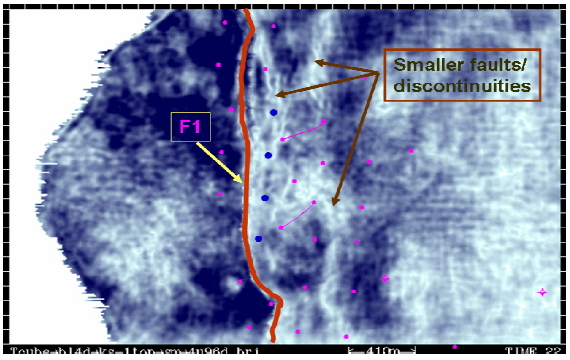

Figure 9: Tuning cube slice at 22 Hz derived along KS-1 top time horizon showing zone of smaller faults.

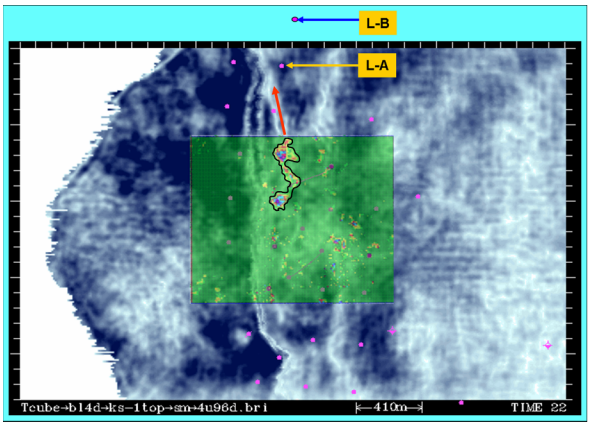

Figure 10: Envelope of time-lapse impedance attribute outlined in black superimposed over Tuning cube slice at 22 Hz derived along KS-1 top time horizon. Probable gas migration path towards north is shown by red arrow.

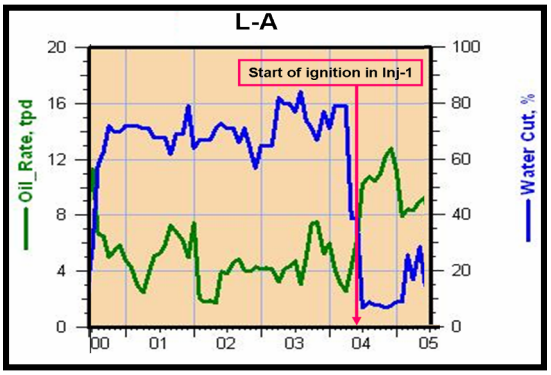

Figure 11: Production profile of well L-A situated north of Inj-1 (see Fig-9 also). The increase in oil rate and decrease in water cut after the initiation of combustion in Inj-1 can be readily seen.

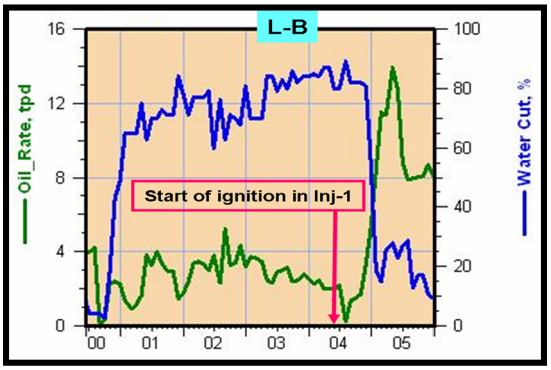

Figure 12: Production profile of well L-B situated north of Inj-1 (see Fig-9 also). The increase in oil rate and decrease in water cut after the initiation of combustion in Inj-1 can be seen.

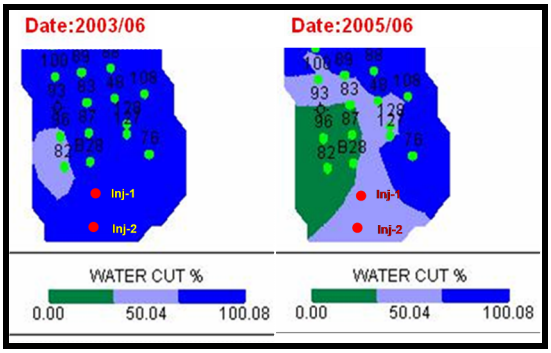

Figure 13: Water cut map of the area north of injectors Inj-1 and Inj-2 based on reservoir engineering data. The decrease in water cut may be attributed to the effect of combustion/injection in the southern part of the area.

Conclusions

The study demonstrates the need of cross-matching the time-lapse datasets prior to an appropriate inversion method to extract a meaningful 4D impedance response. The results of various post-stack inversion workflows applied on time-lapse datasets of Balol Field are clearly non-unique and underlines the inherent non-uniqueness of inversion methods. However, model-based inversion of time-lapse processed datasets has successfully brought out 4D impedance anomalies around injector wells due to in-situ combustion process. The extent of combustion can be estimated from the sizes of these individual time-lapse anomalies around the wells.

Spectral decomposition together with 4D impedance attribute suggests that several smaller faults/discontinuities present in the study area might be acting as the conduits or fairways for the preferential transmission of the thermal energy provided by the in-situ combustion. This presumably has resulted in increased production and decreased water cut in some of the wells located closer to the fairways in the north as observed in reservoir/production behavior of these wells. The study indicates that the most of the flue gases are preferentially moving towards north through the finer N-S discontinuities or high permeability fingers.

References

Asit Kumar and Shyam Mohan, 2004, Feasibility assessment of a time-lapse seismic survey for thermal EOR in Balol Field, India based on rock physics and seismic forward modeling: Proc. 5th Intl. Conference & Exposition on Petroleum Geophysics, SPG, Hyderabad, India, pp 688-695.

Asit Kumar, N. Bhattacharyya and Shyam Mohan, 2006 Cross-equalization for Time-lapse Study in Balol Field, India : Proc. 6th Intl. Conference & Exposition on Petroleum Geophysics, SPG, Kolkata, India, pp

Buland, Arild and Ouair, Youness El, 2006, Bayesian time-lapse inversion, Geophysics, 71, pp R43-48.

S. Gluck*, B. Deschizeaux, A. Mignot, C. Pinson, CGG, F. Huguet, GDF, 2000, Time-lapse impedance inversion of post-stack seismic data: Ann. Intl. Mtg. SEG, Expanded Abstracts.

Landro, 2006, Future challenges and unexplored methods for 4D seismic analysis, CSEG Recorder, Spl. Ed., pp128-135.

Sarkar, Sudipta, 2003, On the inversion of time-lapse data: Ann. Intl. Mtg. SEG, Expanded Abstracts.

Acknowledgments

The views expressed in this paper are those of authors only. The authors would like to acknowledge the support and permission of Oil and Natural Gas Corporation Limited for this work. The authors wish to thank Mr. Sidhartha Sur, GM (Reservoir) for many fruitful discussions and acknowledge Mr. S. K. Sinha and Mr. H. S. Dayal of Heavy Oil Development Group for valuable inputs for this study. The authors express their sincere thanks to Dr. R. V. Marathe, GGM-Head, Institute of Reservoir Studies, Ahmedabad for giving encouragement as well as providing necessary infrastructure to carry out this work and according permission to present/publish this work.